Load bearing, compliant manipulator using non-linear frictional elements

Richard Wakeling-Gentle[1] and Andrew T. Conn[2]

***Abstract*— Tendon driven continuum manipulators have advantages such as being able to deform around and through their environment, but this typically comes at the cost of reduced precision and load bearing capabilities. This paper presents a strong, compliant manipulator system using a rigid-link tendon driven manipulator controlled by a novel compliant drive mechanism. Numerical simulations show that this new manipulator can help to address the stiffness/compliance trade-off by exploiting a compliant drive and a stiff manipulator at the same time. A proof-of-principle real-world prototype demonstrates how the manipulator's compliance enables conformation to the shape of a soft and compressible object while its stiffness can support an object more than 15 times its own weight.**

I. Introduction

Continuum manipulators have been widely investigated and developed in robotics due to their adaptability to different object types and ability to operate in cluttered environments [1]. The central design principle is a slender manipulator capable of a continuous bending motion and of adapting its shape to its environment. Continuum manipulators are commonly made from either a continuous piece of deformable material [2] or a series of rigid links connected by revolute joints [3] and they can feature a wide array of actuation methods, including pneumatic [2] and tendon driven [4] solutions.

Similar to soft robots, continuum manipulators have the ability to perform complex tasks in uncertain environments, such as deforming themselves to conform to their environment, whilst using under-actuating, low dimensional control inputs [5]. However, such robots generally achieve these properties by sacrificing precision and reducing stiffness and load bearing capabilities, when compared to their rigid robot counterparts [6].

Tendon driven, rigid link manipulators are generally characterised by compliant joints and under-actuated control, meaning they have fewer actuators than joints [3], [7]. This active field of research has led to solutions including intricate control methodologies and sensor integration [8]; this paper focuses on the opportunities for increased strength in manipulators with low-dimensional input and minimal control algorithm requirements.

In this paper, a Friction Actuated Load-bearing COmpliant Manipulator (FALCOM) is described, shown in Fig. 1, which is comprised of an under-actuated rigid-link manipulator with a separate tendon for each joint and a torque-limited compliant drive mechanism. This drive mechanism has a single motor and reduces actuator and control complexity by integrating passive frictional elements to rotate tendon spools. This arrangement has the key advantage that if the drive system is locked via a single clutch, the manipulator can behave as a fully actuated system and take advantage of its material strength to resist large external forces.

Compliance is widely regarded as an important safety feature when operating a robot around humans [9], but there are applications such as patient-carrying [10] which require both a high load bearing capacity and direct, safe human-robot interaction.

This paper is arranged as follows: in section II the manipulator design is introduced and the compliant drive mechanism is described, section III describes the dynamic simulation model of the manipulator system, sections IV and V present results generated by this simulation and section VI describes

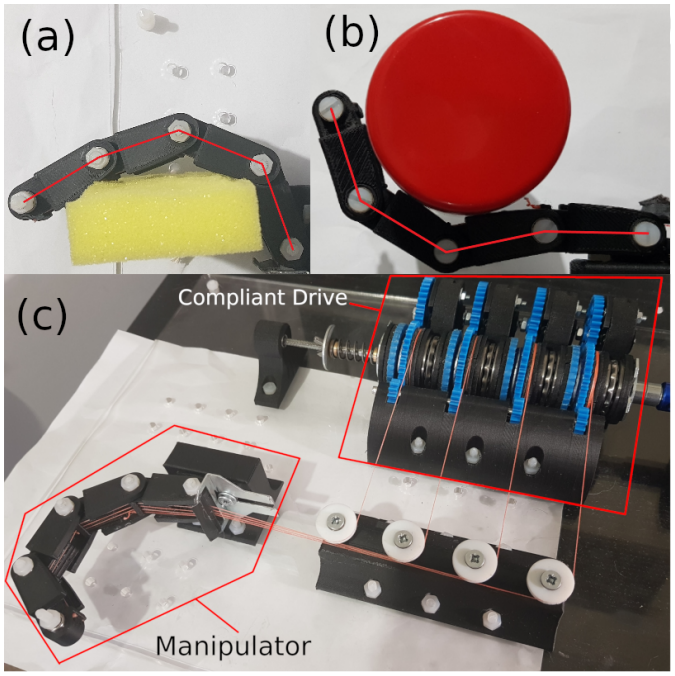

Fig. 1: (a) & (b) :Prototype manipulator (a) gently complying to a sponge (viewed from above), (b) suspending a 500g mass (viewed from the side). Straight red lines overlaid on links for clarity. (c): Overview of prototype manipulator with high-level annotations. See section VI for more detail.

This work was partially funded by EPSRC grants EP/L015293/1 and EP/R02961X/1.

[1]Richard Wakeling-Gentle is with the FARSCOPE CDT at the Bristol Robotics Lab, Bristol, UK richard.wakeling-gentle@brl.ac.uk

[2]Andrew T. Conn is with the Department of Mechanical Engineering, University of Bristol, Bristol, UK and with Bristol Robotics Lab, Bristol, UK a.conn@bristol.ac.uk

real-world testing using a prototype of the compliant drive mechanism.

II. System design

A. Manipulator

The manipulator in this work has a chain-link design, which consists of a series of rigid links connected by one-dimensional revolute joints.

Each joint of these manipulators has a tendon to actuate it, attached to the far end of its distal link. These tendons are routed back along the length of the manipulator and into the compliant drive mechanism discussed in section II-B.

The manipulators used to test the compliant mechanism have either 4 or 5 links, with joints which are 30mm and 20mm apart respectively (measured centre-to-centre).

B. Compliant drive

This section describes how the FALCOM can exhibit both under-actuated compliant behaviour and fully actuated load bearing capabilities. The core of this design is a series of slip-type torque limiters which rely on friction to transfer torque from the driving axle to the spools themselves. Fig. 2 shows a simplified schematic of one such torque limiter set up to drive a single spool.

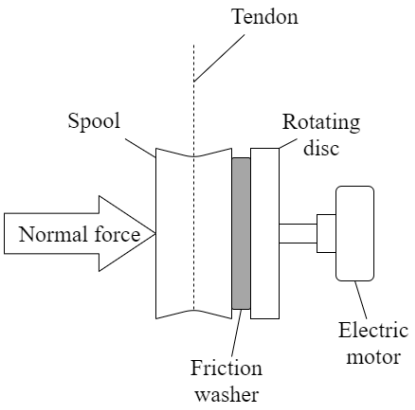

Fig. 2: Torque limited tendon actuator spool.

Consider the system shown in Fig. 2; in the case where the motor turns anti-clockwise (to wind in the tendon), only the rotating disc is driven directly by the motor; it is the friction washer between the disc and the spool that transfers the torque to the spool and winds the tendon in. If the tendon were locked in place by an external force, the motor and the disc would continue to turn, but the torque generated by the friction washer would not be able to turn the spool; the tendon would remain under tension but would not move. This is what generates the compliant behaviour, since the joint actuated by that tendon will slow or stop if it encounters a resisting force in its environment, exerting only a small amount of force generated by the slipping friction washer.

The proposed drive system is comprised of a number of these torque limited spools, with one spool per joint in the actuated manipulator. These spools are arranged in parallel along a single motor-driven axle, with axial bearings between them to ensure that they can rotate freely against each other with minimal friction. Because slowing or stopping a single tendon does not prevent the motor from turning, or affect any of the other spools, the remaining spools are still driven by the motor and can continue actuation of the manipulator. Fig. 3 shows a schematic of this drive layout.

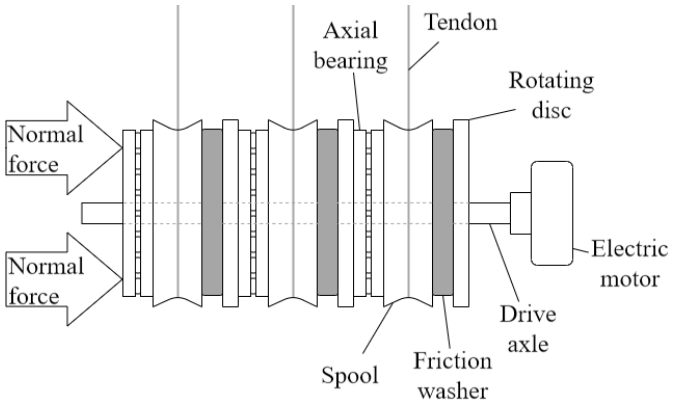

Fig. 3: Schematic of an example compliant drive system with 3 spools, for a 3 joint manipulator.

All of the rotating disks are rotationally coupled directly to the drive shaft and turn with it, while everything else is free to turn about the drive axle. Only the bottom rotating disc and the motor are constrained axially on the shaft, everything else is free to move, except that the normal force from the end opposite the motor will act to keep everything in situ. Because each spool set-up is the same, it is assumed that the normal force will distribute evenly amongst all of the friction components.

C. One-way clutch

The enhanced load bearing capacity of the proposed system relies on the tendons each being able to hold their respective links in position when an external force tries to push the manipulator out of the way. With just the torque limited spools (Fig. 2), the torque limiters will slip and allow the tendons to be drawn out if pulled; this kind of back-driving, whilst helpful for compliance, will cause the manipulator to drop any heavy loads it attempts to carry.

To prevent this back-driving, a one way clutch assembly is coupled with each spool by the means of simple gearing. Each clutch can be enabled and disabled with a mechanical switch and when enabled, only allows its coupled spool to rotate in the direction that winds its tendon in.

III. Simulation design

A dynamic model of the manipulator and its environment was developed to investigate its dynamic response using MATLAB 2021b Simscape Multibody [11], with the Multibody Contact Forces Library [12], Multibody Multiphysics Library [13] and Multibody Parts Library [14] packages.

A. Friction

Friction in the slip-type torque limiters is the key element that governs the behaviour of the proposed manipulator system (see II-B). As such, the equations that describe it are a key part of the system's simulation.

Friction is defined in two parts, static and dynamic; in each case, friction acts to oppose the motion of bodies sliding against each other and is proportional to the normal force pushing them together.

Static friction occurs when objects are in contact with, and at rest relative to, each other (within a small velocity range).

For any given system, there is a maximum static friction force - the breakaway force - that opposes external forces to keep the system at rest. If this force is overcome the bodies begin to slide against one another, but remain in the static friction regime until the breakaway velocity is reached.

When transitioning into dynamic friction, the friction force spikes upwards before decaying exponentially in what is known as the Stribeck effect [15]. Once in the dynamic friction regime, the forces are governed by Coulomb friction, which is constant, and viscous friction, which is proportional to the relative velocity of the sliding bodies.

This simulation uses rotational friction blocks from the ForcesPS library (included with the Multibody Multiphysics library [13]) to calculate friction torque. The equations contained therein require four primary parameters,

T_{brk} = Breakaway torque,
ω_{brk} = Breakaway angular velocity,
T_{Coul} = Coulomb friction torque and
f = Viscous friction coefficient,

from which the secondary parameters

$\omega_{St} = \omega_{brk}\sqrt{2}$ (Stribeck friction velocity threshold) and
$\omega_{Coul} = \omega_{brk}/10$ (Coulomb friction velocity threshold)

are calculated. With these parameters in place, the transferred torque T is calculated as a function of ω:

$$T(\omega) = f\omega + T_{Coul}\tanh\left(\frac{\omega}{\omega_{Coul}}\right) + \frac{\omega}{\omega_{St}}\sqrt{2e}(T_{brk} - T_{Coul})e^{-\left(\frac{\omega}{\omega_{St}}\right)^2}. \quad (1)$$

B. Manipulator

In simulation, manipulator has 5 links, with 20mm between the joints; the main body of each link is formed by two outer plates, connected by the axles of the rotary joints on either end. There is also a force sensor that is the same shape as the main body plates, positioned in the centre of the link. Fig. 4 shows an annotated image of two such links above an image of the whole manipulator.

Actuation is achieved with 5 tendons, each of which is connected to the distal end of one link to provide actuation, and routed back around each of the rotary joints to keep it flush with the manipulator as it moves. The tendons and the pulleys used to route them are sourced from the Belts & Pulleys library included within Simscape Multibody [11].

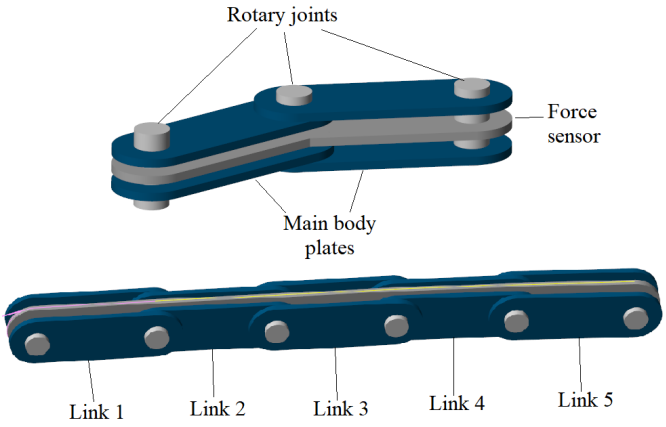

Fig. 4: Annotated image showing the various parts of two manipulator links and the full manipulator laid out in its base configuration.

C. Compliant drive

Having been routed past the base of the manipulator, each tendon is attached to its own spool (again from the Belts & Pulleys library [11]) which is driven by the torque calculated in equation 1. For this calculation, angular velocity ω is determined as the difference between the spool's current velocity ω_s and a constant velocity ω_d representing the motion of the drive shaft,

$$\omega = \omega_d - \omega_s \quad (2)$$

D. One way clutch

Every spool has a uni-directional clutch system attached to it, to prevent back-driving of the tendons.

Each of these clutches is modelled using a unidirectional clutch block and two rotational damper blocks from the Simscape Driveline library (included with Simscape in MATLAB 2021b [11]). The interface between the Driveline and Multibody mechanisms is sourced from the Multibody Multiphysics Library [13].

IV. Simulated Comparison Experiments

The following are a series of simulated experiments comparing the proposed mono-directional complaint manipulator with a single-tendon benchmark manipulator modelled after the literature [7].

The benchmark has the same properties as the simulated FALCOM manipulator (section II-A) except that (a) its joints contain elastic elements and (b) it is actuated by a single tendon attached to the distal end of its furthest link, routed back parallel to the manipulator links and actuated with with a constant velocity.

A. Compliance testing

In order to assess the compliance of the FALCOM, both manipulators were used to grasp the same cylinder, which was fixed rigidly in place. Force measurements were taken for each

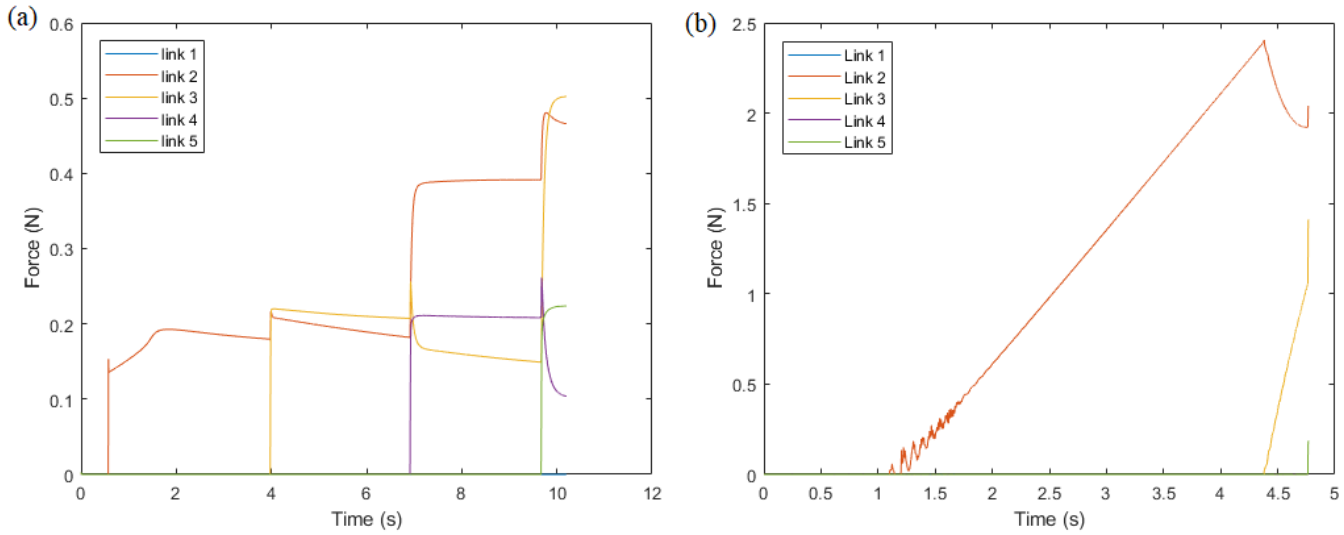

Fig. 5: Force graphs for (a) multi-tendon manipulator design in this work and (b) benchmark single tendon manipulator design from [7].

link to assess compliance, where compliance is determined to be inversely proportional to exerted force.

The input parameters for both of the manipulators were as follows:

Multi-tendon manipulator:

- Breakaway torque (T_{brk}) = 0.01 Nm
- Breakaway angular velocity (ω_{brk}) = 0.1 rad/s
- Coulomb friction torque (T_{Coul}) = 0.008 Nm
- Viscous friction coefficient (f) = 0.02 Nms/rad
- Drive motor speed = 0.4 rad/s
- Spool radius = 0.01 m

Single-tendon benchmark manipulator:

- Joint spring constant = 0.001 Nm/deg (order of magnitude match for that found in [16])
- Drive motor speed = 0.4 rad/s
- Spool radius = 0.01 m

The force data taken from each of the links is presented graphically, for both manipulators, in Fig. 5. The main result of this data is that the maximum force applied by the FALCOM was 0.5N, in comparison to the 2.4N of the benchmark manipulator.

The precise values will change based on input parameters, but these results are sufficient to show that the new manipulator can theoretically match its literature counterparts in terms of grasping compliance.

B. Load bearing test

Assessment of the FALCOM's load bearing capacity was achieved by having it bear the weight of a 1kg cylinder under gravity and observing the motion of both the manipulator and the cylinder over the next 10 seconds. Similarly, the benchmark manipulator was subjected to the same test, again using 0.001 Nm/deg as the joint spring constant.

The FALCOM held the 1 kg cylinder perfectly without moving. On the other hand, the single tendon manipulator dropped the cylinder in less than a second, because its underactuated nature allows it to form into multiple different configurations for the same tendon length. Still images of these simulated experiments are shown in Fig. 6.

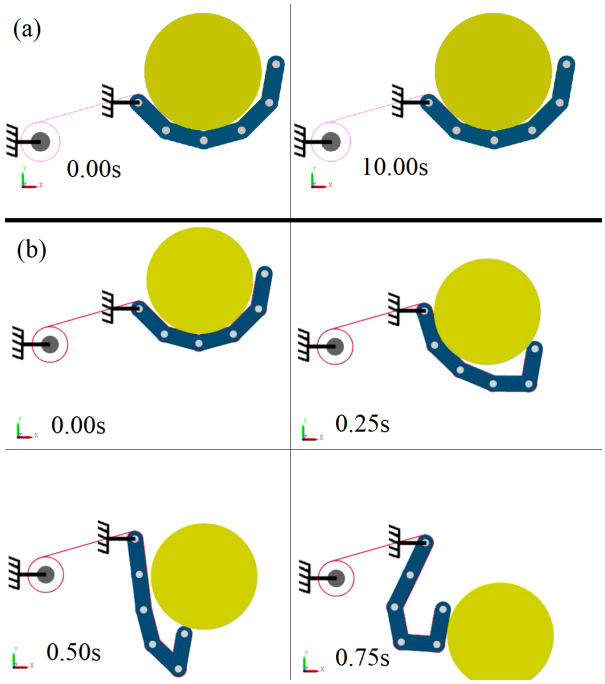

Fig. 6: Still images taken from a recording of (a) FALCOM and (b) benchmark manipulator attempting to support a 1 kg cylinder. (Shown from the side)

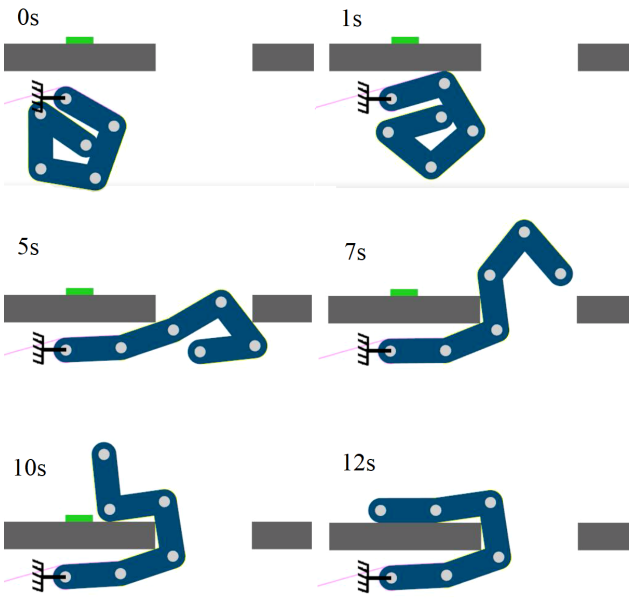

Fig. 7: Time lapse of the manipulator squeezing through a gap and pushing a button on the far side. (Shown from above)

C. Stiffer benchmark

Increasing the benchmark manipulator's spring coefficient to 0.01Nm/deg caused it to suspend the 1kg cylinder in the above load bearing test (section IV-B). However, with this higher spring coefficient, its performance significantly degrades in the compliance experiment from section IV-A, where the maximum force exerted by a single link jumps to from 2.4N to 30N. This highlights the trade-off inherent to single tendon continuum manipulators, which can generally be optimised for either compliance or load bearing capacity.

V. Advanced Compliance

The following simulated experiment was completed with the one-way clutches disabled to allow the manipulator joints to be back-driven, increasing its compliance at the cost of load bearing capacity.

It was discovered that actuating all of the manipulator's tendons at the same rate causes it to maintain its shape until it makes contact with an obstacle. This is particularly useful when starting in a coiled configuration as it allows the manipulator to unfurl over an obstacle, avoiding obstacles which it would hit if it started in a standard, straight configuration. This demonstrates that active switching off the one-way clutches, for example via intermittent actuation from ancillary actuators, allow the FALCOM manipulator to transition between a highly compliant state for navigation through cluttered environments or around fragile objects and a nominal state with compliance in one direction and high stiffness in the other.

Fig. 7 shows a series of still images from a recording of the manipulator unfurling and squeezing through a gap to press a button on the far side of an obstacle.

VI. Prototype Testing

For real-world prototyping, the manipulator was reduced to 4-links, which slightly reduced complexity of construction. Otherwise, the prototype was fabricated to the specifications described in section II, constructed from a combination of PLA 3D printed parts and off-the-shelf components. The manipulator's links were printed as single pieces and are 43mm long (30mm from the centre of one joint to the centre of the next). Once assembled, the manipulator weights 32 grams, including bearings and screws.

Fig. 8 shows an annotated image of the full prototype with the manipulator in its horizontally actuating configuration. An extra set of tendon guides and a different manipulator base can be swapped in to change the manipulator's orientation for vertical actuation.

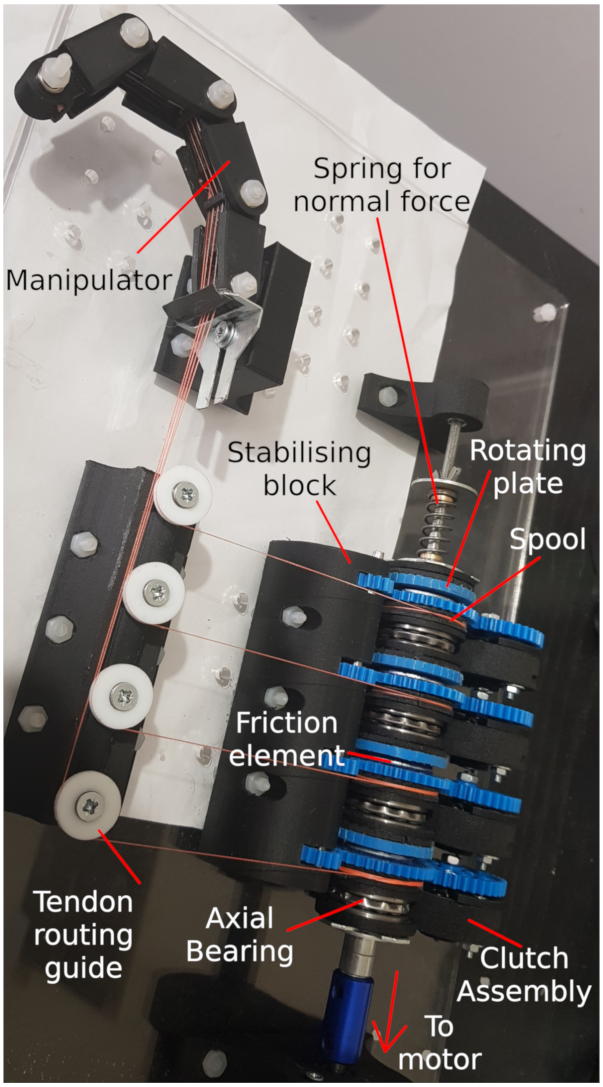

Fig. 8: Annotated image showing the prototype manipulator as a whole, with key components labelled.

A. Simulation verification

As an initial test to verify that the prototype was a behavioural match for the simulation, said simulation was updated to include a 3D model of the real, 3D printed manipulator and both simulated and real manipulators were used to grasp cylindrical objects of diameter 55.3mm.

Fig. 9 shows images of the final positions for simulated and prototype manipulators, Fig. 10 shows plots of the simulated joint angles throughout this task, overlaid onto scatter plots of the prototype's joint angles; prototype joint angles were measured manually from a video file.

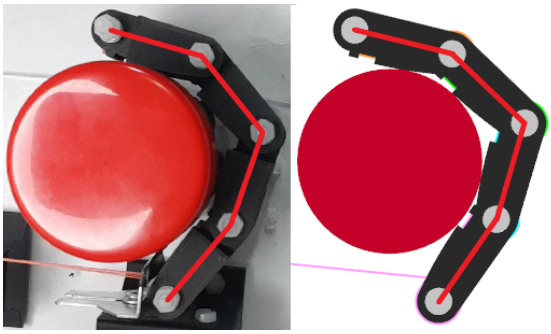

Fig. 9: Prototype (left) and simulated (right) manipulators complying to cylindrical objects. Straight red lines overlaid on links for clarity. Shown from above.

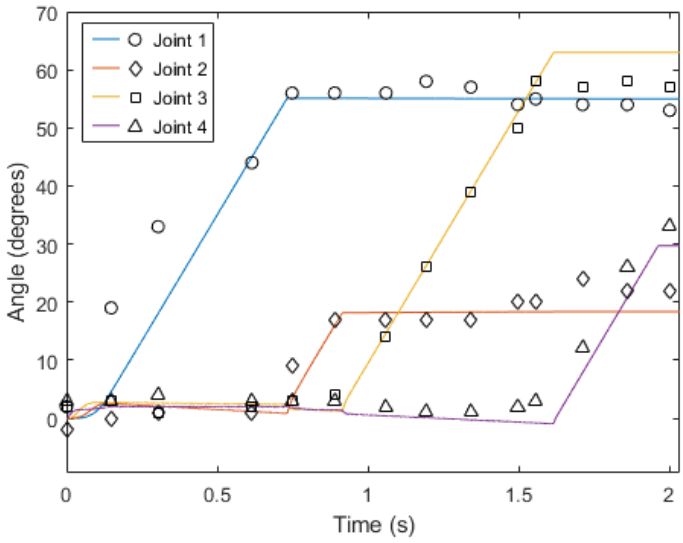

Fig. 10: Comparison of simulated joint movement (lines) to prototype joint movement (symbols) for the compliance task in Fig. 9.

B. Compliance test

The prototype FALCOM was designed to have a variable normal force exerted on the friction elements between its spools and rotating plates, allowing for a variable level of grasping compliance. For this test, the normal force was set at its minimum viable value of ≈9N; any lower and the drive fails to overcome internal friction in the tendon routing system and manipulator joints.

The manipulator was set up such that it actuated in a horizontal plane, to eliminate an uneven influence of gravity between complaint and load bearing directions, and it was driven to grasp an ordinary kitchen sponge, which was rigidly attached to the work bench below it.

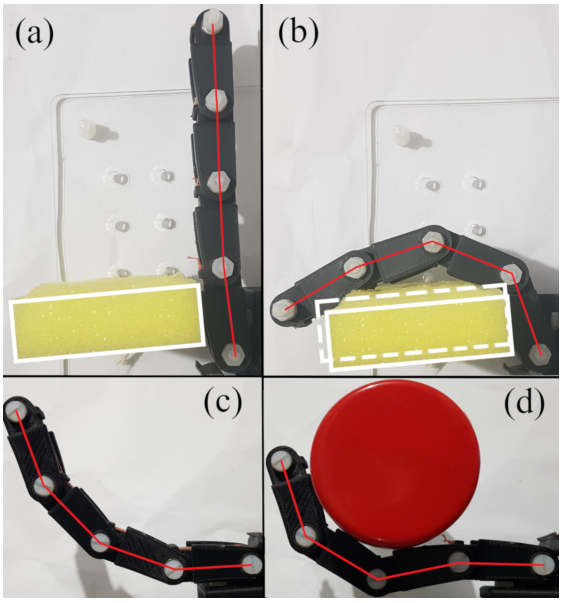

Fig. 11: (a) and (b) show the FALCOM before & after complying to a sponge (shown from above). (c) and (d) show it before & after being loaded with a 500g weight (shown from the side). Straight lines overlaid between joints & around sponge perimeter for clarity.

Fig. 11 (a) & (b) show that the sponge barely moved when grasped by the FALCOM - solid white lines highlight the sponge's location in each image, dashed white lines in (b) show where the sponge was before the manipulator touched it. Since sponges are renowned for their softness, this test demonstrates the manipulator's ability to apply a very low force during a compliance task.

C. Load bearing

In this test, the manipulator was oriented such that it actuated vertically, its tendons were wound in such that it was slightly curved (Fig 11(c)) and the compliant drive was set to ≈9N normal force, the same as the compliance test in VI-B. A 500g mass was placed onto the manipulator to test its load bearing capacity. The manipulator's curvature while loaded is shown in Fig 11(d).

These images show a significant change in the manipulator's curvature, which does not match the simulation prediction of no movement (section IV-B). This discrepancy is caused by limitations in the material strength of the prototype itself; analysis of the prototype yielded the following three sources of

additional compliance, which lowered the manipulator's load bearing capacity:

- Flexion in the steel shaft that holds the spools and rotating plates,
- Flexion of PLA 3D printed parts,
- Stretching of the manipulator's tendons.

Solving any of these issues would increase the load bearing capacity of the manipulator, up to the point where a different limiting factor is reached. The flexion of the steel shaft has been partially solved by the introduction of a stabilising block which coulpes with the spool gears to prevent lateral flexion (Fig. 8); the shaft still flexes downwards, however.

VII. Discussion

This paper described the simulation and prototyping of a novel friction actuated, load-bearing compliant manipulator (FALCOM). This manipulator displays very high compliance in its grasping direction - capable of complying to a sponge with minimal deformation - whilst simultaneously resisting back-driving external forces.

The FALCOM sets itself aside from other rigid link, tendon driven complaint manipulators by displaying these properties without requiring any sensor integration or complex control. The FALCOM requires only a single motor to close, which does not need to be deactivated once a grasp is complete.

The extra compliance demonstrated by the prototype FALCOM leads to the possibility that some compliance can be built into the clutch systems on a link-by-link basis if desired. For example, when carrying something fragile that might move or change shape during transport, it may be beneficial for the distal manipulator links to be able to accommodate some movement to avoid damage while the proximal links remain rigidly constrained to support their load.

In any case, any undesired compliance when back-driving can be eliminated with careful consideration of materials & methods used in construction.

It is worth noting that the FALCOM's compliance in the grasping and back-driving directions are largely independent of each-other. Grasping compliance is controlled by the friction force in the torque limiters whilst resistance to back-driving is dominated by the material construction of the device as a whole.

Potential applications for the device are wide ranging, examples include:

- industrial grasping tasks where the grasped object is not clearly defined beforehand,
- nursing robots which safely carry patients,
- prosthetic gripper which can gently grasp a cup or carry a heavy suitcase with no change in its settings.

Subsequent work would look towards adding extra actuators to toggle one-way clutches and to re-open the manipulator once a grasping task is complete.

Toggling the clutches on and off could be achieved with readily available technology such as servo motors or shape memory alloy components [17].

References

[1] I. D. Walker, "Continuous Backbone "Continuum" Robot Manipulators," *ISRN Robotics*, vol. 2013, pp. 1–19, 2013.

[2] L. A. Al Abeach, S. Nefti-Meziani, and S. Davis, "Design of a Variable Stiffness Soft Dexterous Gripper," *Soft Robotics*, vol. 4, no. 3, p. 44, 2017.

[3] S. Hirose and Y. Umetani, "The development of soft gripper for the versatile robot hand," *Mechanism and Machine Theory*, vol. 13, no. 3, pp. 351–359, 1978.

[4] M. E. Giannaccini, I. Georgilas, I. Horsfield, B. H. P. M. Peiris, A. Lenz, A. G. Pipe, and S. Dogramadzi, "A variable compliance, soft gripper," *Autonomous Robots*, vol. 36, no. 1-2, pp. 93–107, jan 2014.

[5] D. Rus and M. T. Tolley, "Design, fabrication and control of soft robots," *Nature*, vol. 521, no. 7553, pp. 467–475, may 2015.

[6] J. Hughes, U. Culha, F. Giardina, F. Guenther, A. Rosendo, and F. Iida, "Soft manipulators and grippers: A review," *Frontiers Robotics AI*, vol. 3, no. NOV, pp. 1–12, 2016.

[7] I. Hussain, G. Salvietti, M. Malvezzi, and D. Prattichizzo, "On the role of stiffness design for fingertip trajectories of underactuated modular soft hands," in *Proceedings - IEEE International Conference on Robotics and Automation*, 2017, pp. 3096–3101.

[8] W. Friedl and M. A. Roa, "CLASH—A Compliant Sensorized Hand for Handling Delicate Objects," *Frontiers in Robotics and AI*, vol. 6, no. January, pp. 1–15, 2020.

[9] H. Abidi and M. Cianchetti, "On Intrinsic Safety of Soft Robots," *Frontiers in Robotics and AI*, vol. 4, p. 5, 2017. [Online]. Available: https://www.frontiersin.org/article/10.3389/frobt.2017.00005

[10] Y. Liu, G. Chen, J. Liu, S. Guo, and T. Mukai, "Biomimetic Design of a Chest Carrying Nursing-Care Robot for Transfer Task," in *2018 IEEE International Conference on Robotics and Biomimetics (ROBIO)*, 2018, pp. 45–50.

[11] Mathworks Inc., "MATLAB 2021b," 2021. [Online]. Available: https://uk.mathworks.com/products/matlab.html

[12] S. Miller, "Simscape Multibody Contact Forces Library," 2021. [Online]. Available: https://github.com/mathworks/Simscape-Multibody-Contact-Forces-Library

[13] ——, "Simscape Multibody Multiphysics Library," 2021. [Online]. Available: https://github.com/mathworks/Simscape-Multibody-Multiphysics-Library

[14] ——, "Simscape Multibody Parts Library," 2021. [Online]. Available: https://github.com/mathworks/Simscape-Multibody-Parts-Library

[15] E. Pennestrì, V. Rossi, P. Salvini, and P. P. Valentini, "Review and comparison of dry friction force models," *Nonlinear Dynamics*, vol. 83, no. 4, pp. 1785–1801, 2016.

[16] I. Hussain, G. Salvietti, G. Spagnoletti, and D. Prattichizzo, "The Soft-SixthFinger: a Wearable EMG Controlled Robotic Extra-Finger for Grasp Compensation in Chronic Stroke Patients," *IEEE Robotics and Automation Letters*, vol. 1, no. 2, pp. 1000–1006, jul 2016.

[17] J. L. Lemanski, V. B. Krishnan, R. M. Manjeri, W. U. Notardonato, and R. Vaidyanathan, "A low hysteresis NiTiFe shape memory alloy based thermal conduction switch," *AIP Conference Proceedings*, vol. 824 I, no. April 2006, pp. 3–10, 2006.